

A near and far-field monitoring technique for damage detection in concrete structures

Costas Providakis^{*1}, K. Stefanaki¹, M. Voutetaki¹, J. Tsompanakis²
and M. Stavroulaki¹

¹*Applied Mechanics Lab, School of Architectural Engineering, Technical University of Crete, GR-73100 Chania, Greece*

²*School of Environmental Engineering Technical University of Crete, GR-73100 Chania, Greece*

(Received April 12, 2014, Revised May 4, 2014, Accepted May 8, 2014)

Abstract. Real-time near and far-field monitoring of concrete structural components gives enough information on the time and condition at which damage occurs, thereby facilitating damage detection while in the same time evaluate the cause of the damage. This paper experimentally investigates an integrated monitoring technique for near and far-field damage detection in concrete structures based on simultaneous use of electromechanical admittance technique in combination with guided wave propagation. The proposed sensing system does not measure the electromechanical admittance itself but detect time variations in output voltages of the response signal obtained across the electrodes of piezoelectric transducers bonded on surfaces of concrete structures. The damage identification is based on the spectral estimation MUSIC algorithm. Experimental results show the efficiency and performance of the proposed measuring technique.

Keywords: electromechanical admittance; guided waves; concrete beam structures; PZT patches; chirp signal; fourier transform

1. Introduction

The structural integrity of the civil infrastructure is very important for the safety, productivity and quality of life of the society. This integrity is often a concern due to the aging of the infrastructure, the occurrence of earthquakes, exposure to wind loading and ocean waves, soil movement, excessive loading and temperature excursions. Thus, there is need for real-time monitoring damage in a non-destructive way, so that timely repair or retirement of structures takes place.

Damage sensing (i.e., structural health monitoring) is valuable for concrete structures for the purpose of hazard mitigation. Health of concrete structures is mainly monitored by recording and measuring propagation of stress waves through them. The occurrence of damage generates changes of stress waves which carry important information of the nature and extent of damage. This allows for a reduction of the cost of maintenance and inspection tasks leading to a more

*Corresponding author, Professor, E-mail: cprov@mred.tuc.gr

economical condition-based maintenance strategy that is capable of prompt condition assessment of critical civil facilities.

Many traditional global or local experimental structural health monitoring (SHM) and damage detection methods have been proposed in the past and have been used in a variety of concrete structures such as C-scan, X-rays, radar techniques, etc (Cruz *et al.* 2010, Fan and Qiao 2011, Brownjohn *et al.* 2011). While these techniques provide useful information for the decision makers, however, they require bulky equipments, they are extremely time-consuming and most of them request that the vicinity of the damage is known a priori.

One of the promising active sensing approaches which utilizes piezoelectric (PZT) transducers as actuators/sensors, the electromechanical admittance, or its inverse impedance, the so-called EMA technique, has received growing attention in recent years for in-situ health monitoring due to its distinct advantages (Annamdas and Soh 2010, Kumar *et al.* 2012, Yun *et al.* 2011). EMA response is derived from the dynamic interaction between PZT transducers and the host structure. EMA is typically applied using an electrical impedance analyser which scans a predefined frequency range in the order of tens to hundreds of kHz. The main advantage of EMA technique is its capability to detect local (near-field) damages, even in complex structures. However, unfortunately, taking into account that since steady-state response, which is needed for admittance measurements, is limited to a small region close to the admittance transducer one may conclude that EMA can detect damages only locally. In contrast, when guided stress wave (Raghavan and Cesnik 2007) is propagated along the length of any structural component then the boundary of the components allow a long range "guidance" achieving far-field monitoring capabilities.

In the present paper, the proposed damage detection technique does not use any measurement of the electromechanical admittance itself. The conventional admittance sensing technique is replaced here by acquiring output voltage variations generated across a simple circuit connected to the PZT transducer. To combine the advantages of EMA and GW techniques an integrated multi-mode sensing technique is proposed, referred as EMA-GW technique (Providakis *et al.* 2012) that detects changes in the admittance spectrum of a PZT transducer in the range of a predefined frequency band as generated by: a) continuous locally inspected admittance signatures, and b) simultaneously detected changes in admittance signatures from guided wave disturbances originated from a second PZT patch which acts as a guided wave transmitter.

The main advantage of the proposed approach is that the combined EMA-GW technique incorporating synchronous admittance-based and guided wave propagation measurements retains the benefits of both techniques allowing effective near-field damage detection and in the same time increased sensing capabilities for wider regions. The combine use of the two techniques has been also investigated by other researchers over the last decade (Georgiutiu *et al.* 2004, Wait *et al.* 2005, Park *et al.* 2006, Zagari *et al.* 2010, An and Sohn 2011, Park *et al.* 2012, An *et al.* 2012, Zhu and Rizzo 2012, Dürager *et al.* 2012), however, the applicability of those techniques has not yet been tested or demonstrated in details for concrete structures. For instance, in the monitoring technique presented in the recent work of Zhu and Rizzo (2012), an integrated experimental monitoring procedure was demonstrated dealing only with Lamb wave propagation in steel structures.

To detect damage in a concrete structure, it is necessary to develop a damage identification methodology that can extract the quantitative information of any damage state affecting the performance of the structure. The damage identification using electromechanical admittance measurements is a complicated procedure since it is embedded in high-level noise. Therefore, to have a reliable data analysis tool capable of analyzing damage in concrete structures with low

signal-to-noise ratio, a high-resolution spectral estimation through the multiple signal classification (MUSIC) algorithm (Jiang and Adeli 2007) is implemented.

Experimental implementations of the proposed integrated measuring system prove that the present system is effective and reliable to detect near and far-field damage conditions of concrete structural components.

2. The concept of integrated electromechanical EMA-GW monitoring approach

For the proposed integrated EMA-GW approach, the simultaneous activation of electromechanical admittance measurements and guided wave excitation is needed. In its current prototype version, the proposed integrated system includes at least two PZT transducers. Certainly, for real-life concrete structures applications the proposed system should be extended to an array of PZT transducers. The main idea of the proposed monitoring approach is based on the fact that the same type of PZT transducers could be used as admittance and guided wave actuators/sensors. Thus, activating one PZT (denoted as PZT2 in Fig. 1) transducer, electromechanical admittance changes are acquiring at its electrodes to detect near-field damage. The same PZT could sense any far-field changes that may occur, taking into account guided wave disturbances as excited from the other PZT (PZT1) transducer shown in Fig. 1. PZT1 is used as a guided wave generator by applying waves of voltages at its electrodes, as depicted in the detail of Fig. 1.

The guided wave generated by PZT1 transducer propagates along the concrete structure in a path reaching the damaged area, where a part of the wave would reflect due to damage and another part continues propagating beyond the damage. Subsequently, this guided wave will reach PZT2 admittance sensor, leading to disturbances of acquired admittance signatures.

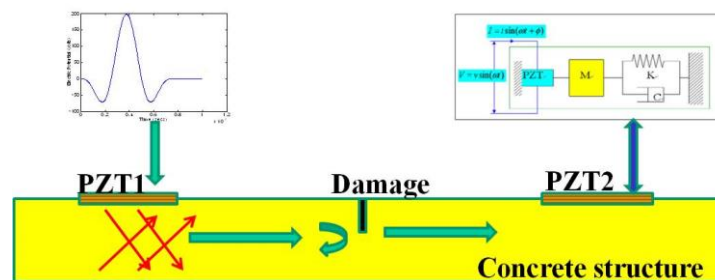


Fig. 1 An overall schematic of the proposed integrated EMA-GW monitoring approach

3. Custom-made sensing system based in integrated EMA-GW technique

A typical circuit that can measure the unknown admittance (or its inverse impedance) across PZT's electrodes uses the I-V methodology [Agilent application note (2000)] where acquisition of voltage and current passing through the PZT is required. The simple circuit shown in Fig. 2 uses a

low value reference resistor (say 378Ω) which is connected in series with the PZT (denoted as PZT2) transducer. To excite the PZT, a National Instruments USB-6251 high-speed M series multifunction data acquisition (DAQ) module is utilized and optimized for accuracy at fast sampling. The excitation voltage V_{in} is of sinusoid-type having an amplitude of $|V_{in}|$ and a frequency sweeping from F_{start} to F_{end} (say 1 kHz to 600 kHz). A two-channel Agilent 2000X oscilloscope was used to record simultaneously the time history of voltage $V_{in}(t)$ at one of the output channels of the USB-6251 card and the time history of voltage drop $V_{out}(t)$ on the calibrated resistor Ref. The current $I(t)$ flowing through the PZT also flows through the resistor R_{ef} .

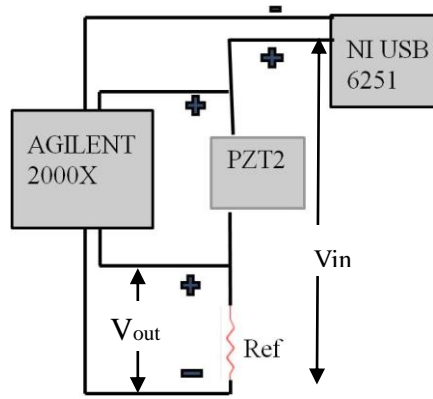


Fig. 2 Simple circuit for electromechanical admittance measurements

If we excite the PZT by a sinusoidal wave the current flow across PZT electrodes is calculated by using the output voltage V_{out} measurement across the reference resistor R_{ef} . In frequency domain the current $I(\omega)$ can be calculated as $I(\omega) = V_{out}(\omega) / R_{ef}$. Hence, the PZT admittance Y in frequency domain is calculated using an expression of the type

$$Y(\omega) = \frac{I(\omega)}{V(\omega)} = \frac{V_{out}}{V_{in}(\omega) - V_{out}(\omega)} * \left(\frac{1}{R_{ef}} \right) \quad (1)$$

Solving Eq. (1) for the output voltage across the resistor $V_{out}(\omega)$ we obtain

$$V_{out}(\omega) = \frac{Y(\omega) * R_{ef}}{(1 + Y(\omega) * R_{ef})} * V_{in}(\omega) \quad (2)$$

Taking into account Eq. (2), one can observe that the output voltage across the resistor in frequency domain is directly related to the electromechanical admittance. Thus, in the subsequent analysis we employ the output voltage V_{out} across the resistor instead of electromechanical admittance itself. To integrate the simple circuit of Fig. 2 to include guided wave capabilities and develop a near and far-field sensing circuit combining electromechanical admittance (EMA) and Guided Wave (GW) methodologies, denoted as EMA-GW, we designed the compact measuring system shown in Fig. 3.

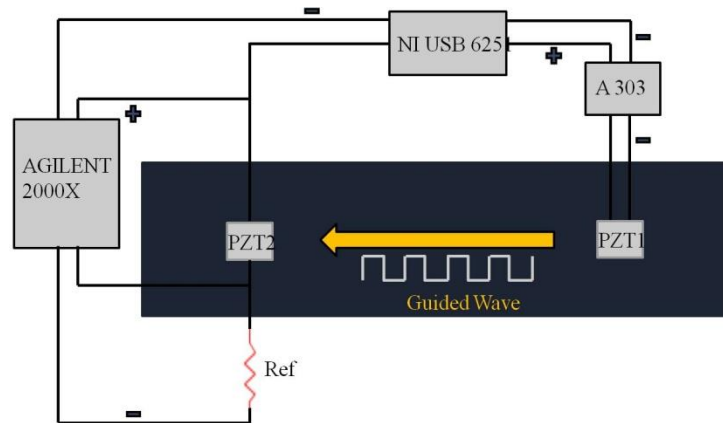


Fig. 3 Proof-of-concept demonstration of integrated measuring system

To achieve a wide band excitation signal sweeping, a digitally synthesized linear chirp signal is generated ($F_{\text{start}}=1$ kHz, $F_{\text{end}}=600$ kHz) by using Labview Signal Express program (Labview 2012) and then transmitted to the admittance measuring circuit by the output channel of USB-6251 card. To create the propagating guided wave, a similar to the first one PZT patch, denoted as PZT1, is also surface bonded on the concrete beam specimen in a distance of 200 mm from the first one. This PZT patch serves as a guided wave actuator by connecting its electrodes to one of the rest output channels of USB-6251 multifunction card. The USB-6251 guided wave output signal was pre-amplified by 20 times using a piezo-driver. A 59 kHz sequence of square guided wave signals, sampled at 1MHz was selected to drive the PZT actuator. The whole experimental arrangement is presented in Fig. 4.

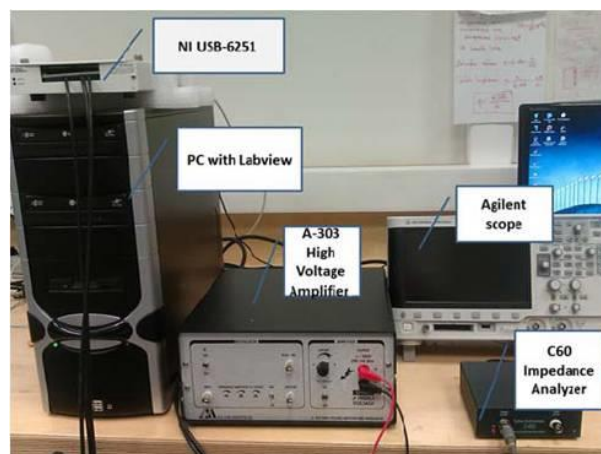


Fig. 4 Experimental arrangement

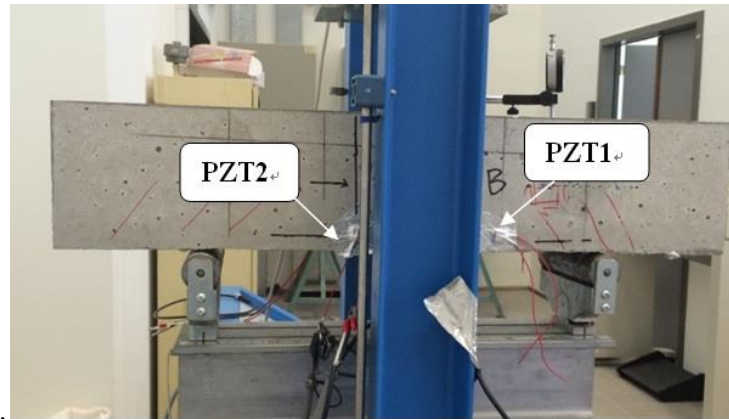


Fig. 5 Concrete beam specimen with surface mounted PZT-based measuring system

4. Experimental setup and loading procedure

Experiments are conducted by surface mounting two PZT patches of type PIC255 (Pi Ceramic 2014) and with a size of $10 \times 10 \times 2 \text{ mm}^3$ at the desired locations of a $150 \times 150 \times 750 \text{ mm}^3$ concrete beam specimen in a setup shown in Fig. 5. The concrete beam specimen is made by a mixing proportion of 1:0.62:2.25:3.83 (Cement: Water: Fine Aggregate: Coarse Aggregate, ratio by mean of cement). In order to protect the electric pole surfaces of PZT transducers from being eroded it is covered with a waterproof tape substance.

The investigated concrete beam specimen was gradually damaged under a 3-point bending test. During the loading procedure, the integrated EMA-GW damage monitoring approach was performed to evaluate the damage status of the concrete beam to detect the existence of cracks. In this experimental program the cracks were caused by 5 loading levels:

- Level 1 : Loading equals to 10 kN
- Level 2 : Loading equals to 20 kN
- Level 3 : Loading equals to 60 kN
- Level 4 : Loading equals to 66 kN
- Level 5 : Loading equals to 68 kN (Failure)

Beam specimen was first evaluated by using the proposed integrated EMA-GW approach at level 1 to establish a baseline. Next, the beam was loaded in a load control mode, up to failure. During the load control process, the load was increased to examine the severity of damage up to the desired level and then reduced to zero and held there constant for a short time interval for data acquisition.

5. MUSIC algorithm applied to identify damage feature

MUSIC algorithm is known as a high-resolution spectrum approach which can detect frequencies with low signal-to-noise ratio assuming that any discrete time signal $x(n)$ can be described by a sum of m complex sinusoid in noise $e(n)$ (Jiang and Adeli 2007). Assuming

$$x[n] = \sum_{i=1}^m \bar{B}_i e^{-j2\pi f_i n} + e[n], \quad n = 0, 1, 2, \dots, N-1 \quad (3)$$

where

$$\bar{B}_i = |B_i| e^{j\phi_i} \quad (4)$$

where N , B_i , and f_i are the numbers of sample data, the complex amplitude and its frequency, respectively, and $e[n]$ is a sequence of white noise with zero mean and a variance σ^2 . This method uses the eigenvector decomposition of $x[n]$ to obtain two orthogonal subspaces. The autocorrelation matrix R of the noisy signal $x[n]$ is the sum of the autocorrelation matrices of the pure signal R_s and the noisy R_n as follows

$$R = R_s + R_n = \sum_{i=1}^P |B_i|^2 e(f_i) e^H(f_i) + \sigma_n^2 I \quad (5)$$

where P is the number of frequencies, the exponent H denotes Hermitian transpose, I is the identity matrix and $e^H(f_i)$ is the signal vector given by

$$e^H(f_i) = [1 e^{-j2\pi f_i}, \dots, e^{-j2\pi f_i(N-1)}] \quad (6)$$

From the orthogonality condition of both subspaces, the MUSIC pseudospectrum Q of the current space vector is given by

$$Q^{MUSIC}(f) = \frac{1}{|e(f)^H V_{m+1}|^2} \quad (7)$$

where V_{m+1} is the noise eigenvector. This equation exhibits the peaks that are exactly at frequency of principal sinusoidal component, where $e(f)^H V_{m+1} = 0$. In the present paper, the MUSIC algorithm is applied in the special case of $m=P+1$, i.e., only the lower eigenvalue is associated to noise.

6. Damage identification and experimental verification

To experimentally validate the proposed multi-mode integrated monitoring technique we monitor the concrete beam specimen shown in Fig. 5. The proposed damage detection approach consists of two basic steps: a) MUSIC pseudospectra of the response voltage V_{out} will be acquired for one of the PZT patches (say PZT2) by using the custom made admittance measuring circuit activated by the linear chirp described in Eq. 8(b) in the same time, the other PZT patch (say PZT1) is excited by the National Instrument USB-6251 unit running under NI Labview Signal Express in such a way that in one of its output ports generates a 59kHz sequence of 10V peak-to-peak square guided waves

$$V_{in} = \sin\left(2 * \pi * \frac{F_{start} * t + (F_{end} - F_{start}) * t * t}{samples * \left(\frac{1}{F_s}\right)}\right) \quad (8)$$

The MUSIC algorithm of MATLAB Signal Processing Toolbox (MATLAB (20012)) is

employed to compute the V_{out} pseudospectra values of the highest peak amplitudes, denoted as A1 and A2, in the preselected frequency band of 10 kHz to 600 kHz. In Providakis *et al.* (2013), after employing detailed numerical dynamic analyses of free-free PZTs of type PIC 255, we concluded that those A1 and A2 highest amplitudes are located at the resonance frequencies of free-free PZTs around 150 kHz and 350 kHz, respectively, and have superior effect on the dynamic behavior of concrete-PZTs dynamic system. This behavior helped us to assume that two real sinusoidal components are present in the signal subspace according to MUSIC algorithm. In this case, the dimension of the signal subspace in the MUSIC algorithm of MATLAB Signal Processing Toolbox is four because each real sinusoid is the sum of two complex exponents. We also set the value of the length of each of the time-based segments into which the input signal V_{out} is divided to double the number of dimension of the signal subspace. As soon as MUSIC pseudospectra of V_{out} are obtained for the pre-selected frequency bands where there exist the greater energy concentration, a damage identification index value (DIIV) is obtained as the ratio of the pseudospectra amplitude peaks (A1) and (A2) over the main amplitude peak (A1) in the analysis frequency band

$$DIIV=20*\log_{10}(A2/A1) \quad (9)$$

Cracks or damage, inside the concrete beam specimen, act as stress relief in the wave propagation path. The amplitude of the wave and the transmission energy will decrease due to the existence of cracks. The drop in value of the transmission energy is correlated with the degree of the damage inside. The concrete beam specimen which is tested in the present paper was observed to have a shear failure starting from the middle top of the specimen, as shown in Fig. 6 and propagating diagonally up to the right support of the beam specimen. The location of admittance sensor PZT2 is selected to be in a distance of about 300 mm which is far enough from the crack affected area in order to evaluate the sensitivity of PZT2. In contrast, the guided wave actuator PZT1 is instrumented very close to the right support, a location very critical from the point of view of shear cracks. The concrete beam specimen is continuously monitored and observable shear cracks could only be detected at loading Level 2 when a diagonally extended shear crack of 0.1 mm in width is visible.

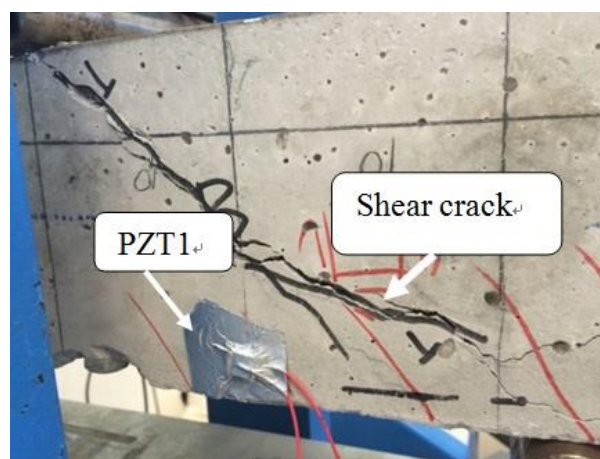
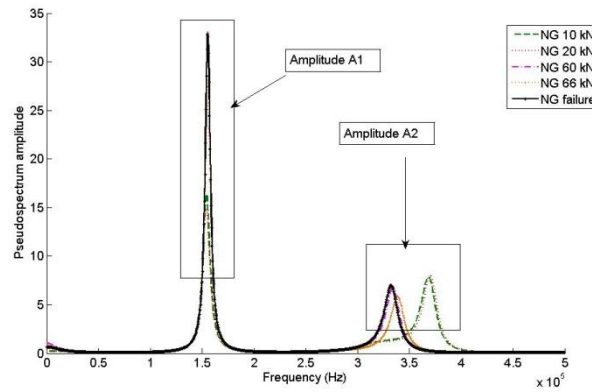
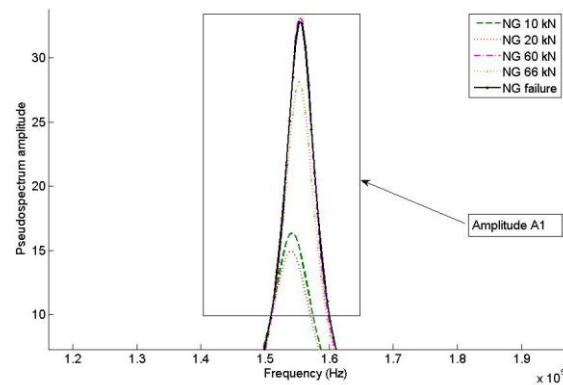


Fig. 6 Severe shear crack observed on concrete beam specimen at Level 4 (66 kN)



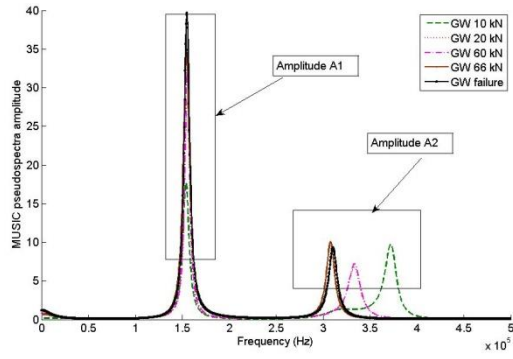
(a)



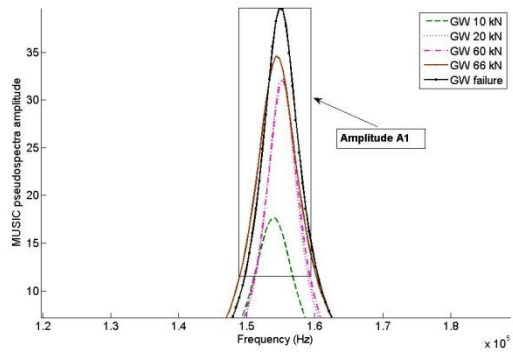
(b)

Fig. 7 (a) MUSIC pseudospectra for the various loading levels without guided waves and (b) Detail for AIMUSIC pseudospectra amplitude for the various loading levels without guided waves

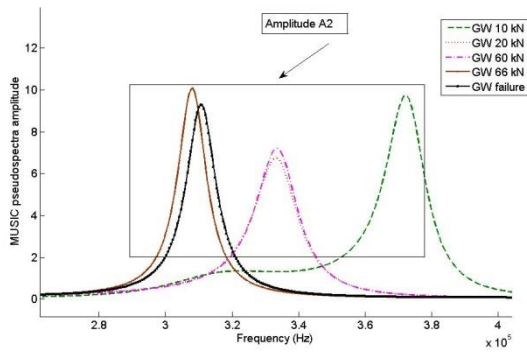
Raw MUSIC pseudospectra signatures of the output voltage generated at the PZT2 surface for the Level 1 (10 kN) to Level 5 (Failure) loading condition when the guided wave generation from PZT1 is active, are depicted in Figs. 7(a) to 7(c). From Level 1 to Level 2, only minor deviations could be noticed in the raw MUSIC signatures, both in amplitude A1 and amplitude A2. A prominent change is presented from Level 3 onwards. However, taking into account that a visible crack of 0.5 mm in width starts already to be observable at previous Level 2, this result prove that the effect of shear damage at the PZT2 output voltage pseudospectrum is not so clearly visible when there is no any guided wave activated from PZT1. This means that the area where the cracks are propagated is located away from the sensing area of PZT2 degrading the capability of EMA measurement in the detection of damage.



(a)



(b)



(c)

Fig. 8 (a) MUSIC pseudospectra for the various loading levels with guided waves and (b) Detail for AIMUSIC pseudospectra amplitude for the various loading levels with guided waves

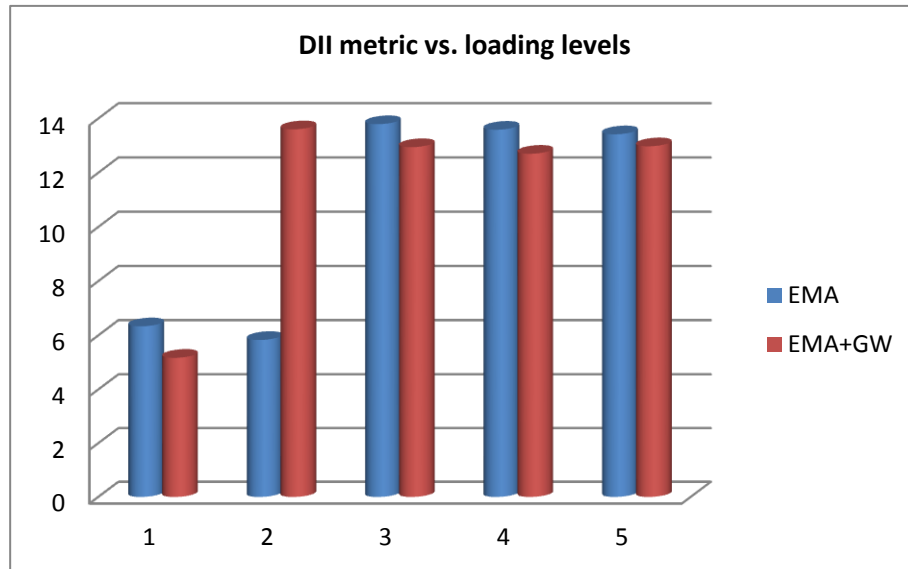


Fig. 9 DII value metric as a function of applied loading levels

Figs. 8(a) to 8(c) show the raw MUSIC pseudospectra signatures of PZT2 patch when the guided wave actuator PZT1 is activated. Taking into account these figures, it is very interesting to show that comparing Level 1 and Level 2 raw signatures, one can observe that the differences in pseudospectrums are more pronounced than those be observed in Figs. 7(a) to 7(c) where the actuator PZT1 was not activated for the same loading levels. A clearly visible shift both in amplitude and frequency is presented at Level 2. This observation is consistent with the fact that the visible crack starts from Level 2 onwards. This means that the introduction of guided wave (EMA+GW) enhance the sensing capabilities of EMA technique.

Fig. 9 compares the computed damage identification index (DII) values at the various loading levels as obtained for both two monitoring cases: a) the conventional technique based on the acquisition of electromechanical admittance (EMA) signatures (or the relative output voltage), and b) the integrated methodology of electromechanical admittance combined with guided wave technique (EMA+GW). By inspecting Fig. 9, a prominent shift of DII value is noticed between level 1 and level 2 loading condition for EMA+GW technique provided damage warning earlier than that resulted from EMA technique itself.

7. Conclusions

In this paper, a new integrated methodology of monitoring and identifying damage in concrete structures is presented. The proposed methodology is based on the electromechanical admittance sensing technique using the output voltage signatures produced across a PZT transducer which is surface bonded on the concrete specimen instead of acquiring the admittance itself. The output

voltage is acquired across a custom-made circuit which greatly simplifies the procedure. This output voltage is appropriately affected by guided wave driven from another PZT transducer which acts as wave actuator. The proposed integrated methodology is effectively applied to detect damage by monitoring changes on the extracted values of a damage metric based on the ratio between amplitudes occurring at peak locations of MUSIC algorithm pseudospectra signatures.

The results demonstrated that the simultaneous consideration of the advantages of the aforementioned damage identification techniques, in a unified but yet effective manner combines the benefits of simultaneous near- and far-field damage detection. Therefore, the proposed technique can be regarded as a simple and practical SHM technique which will help to evaluate the condition of a concrete structure, in order to detect damages early and to make the corresponding maintenance decision for preventing the failure of concrete structures avoiding human and economic loss. Of course, further study should be underway to provide general guidelines and optimize the proposed technique.

Acknowledgements

This research has been co-financed by the European Union (European Social Fund – ESF) and Greek national funds through the Operational Program "Education and Lifelong Learning" of the National Strategic Reference Framework (NSRF) - Research Funding Program: THALES, Investing in knowledge society through the European Social Fund.

The authors would also like to thank Professor Pol Spanos, Rice University, USA, for his valuable suggestions which have made the present research to be successfully performed.

References

- Agilent Technologies (2000), *Application Note 346-4*.
- An, Y.K. and Sohn, H. (2011), "Integrated impedance and guided wave based damage detection under temperature variation", *Proceedings of the SPIE 7981, Sensors and Smart Structures Technologies for Civil, Mechanical and Aerospace Systems*, doi: 10.1117/12.880753.
- An, Y.K., Kim, M.K. and Sohn, H. (2012), "Airplane hot spot monitoring using integrated impedance and guided wave measurements", *Struct. Control Health Monit.*, **19**(7), 592-604.
- Annamdas V.G.M. and Soh C.K. (2010), "Application of electromechanical impedance technique for engineering structures: review and future issues", *J. Intell. Mat. Syst. Str.*, **21**(1), 41-59.
- Brownjohn, J.M.W., de Stefano, A., Xu, Y. L., Wenzel, H. and Aktan, A.E. (2011), "Vibration-based monitoring of civil infrastructure: challenges and successes", *J. Civil Struct. Health Monit.*, **1**(3-4), 79-95.
- Cruz, P.J.S., Topczewski, L., Fernandes, F.M., Trela, C. and Lourenço, P.B. (2010), "Application of radar techniques to the verification of design plans and the detection of defects in concrete bridges", *Struct. Infrastruct. E.*, **6**(4), 395-407.
- Dürager, C., Heinzelmann, A. and Riederer, D. (2012), "A wireless sensor system for structural health monitoring with guided ultrasonic waves and piezoelectric transducers", *Struct. Infrastruct. E.*, doi:10.1080/15732479.2012.671833.
- Georgiutiu, V., Zagrai, A. and Bao, J.J. (2004), "Damage identification in aging aircraft structures with piezoelectric wafer active sensors", *J. Intell. Mat. Syst. Str.*, **15**(9-10), 673-687.
- Jiang, X. and Adeli, H. (2007), "Pseudospectra, MUSIC, and dynamic wavelet neural network for damage detection of highrise buildings", *Int. J. Numer. Meth. Eng.*, **71**(5), 606-629.
- Fan, W. and Qiao, P.Z. (2011), "Vibration-based damage identification methods: a review and comparative

- Study”, *Struct. Health Monit.*, **10**(1), 83-111.
- Kumar, R.P., Oshima, T., Mikami, S., Miyamori, Y. and Yamazaki, T. (2012), “Damage identification in a lightly reinforced concrete beam based on changes in the power spectral density”, *Struct. Infrastruct. E.*, **8**(8), 715-727.
- Labview (2012), *National Instruments*, USA, www.ni.com
- Matlab (2010), *Signal Processing toolbox*, The Mathworks Inc., U.S.A., www.mathworks.com.
- Park, S., Ahmad, S., Yun, C.B. and Roh, Y. (2006), “Multiple crack detection of concrete structures using impedance-based structural health monitoring techniques”, *Exper. Mech.*, **46**(5), 609-618.
- Park, H.J., Sohn, H., Yun, C.B., Chung, J. and Lee, M.M. (2012), “Wireless guided wave and impedance measurement using laser and piezoelectric transducers”, *Smart Mater. Struct.*, **21**(3), 035029, doi: 10.1088/0964-1726/21/3/035029.
- PI Ceramic GmbH (2012), www.piceramic.com, Germany.
- Providakis, C., Stefanaki, K., Voutetaki, M., Tsompanakis, J. and Stavroulaki, (2012), “Damage detection in concrete structures using a simultaneously activated multi-mode PZT active sensing system : numerical modeling”, *Struct. Infrastruct. E.*, doi: 10.108/15732479.2013.831908.
- Raghavan, A. and Cesnik, C.E.S. (2007), “Review of guided-wave structural health monitoring”, *Shock Vib. Dig.*, **39**(2), 91-114.
- Wait, J.R., Park, G. and Farrar, C.R. (2005), “Integrated structural health monitoring assessment using piezoelectric active sensors”, *Shock Vib.*, **12**(6), 389-405.
- Worden, K. (2001), “Rayleigh and Lamb waves – Basic principles”, *Strain*, **37**(4), 167-172.
- Yun, C.B., Lee, J.J. and Koo, K.Y. (2011), “Smart structure technologies for civil infrastructures in Korea: recent research and applications”, *Struct. Infrastruct. E.*, **7**(9), 673-688.
- Zagrai, A., Doyle, D. and Gigineishvili, V. (2010), “Piezoelectric wafer active sensor structural health monitoring of space structures”, *J. Intell. Mat. Syst. Str.*, **21**(9), 921-940.
- Zhu, X. and Rizzo, P. (2012), “A unified approach for the structural health monitoring of waveguides”, *Struct. Health Monit.*, **11**(6), 629-642.